SiliconPV 2025, 15th International Conference on Crystalline Silicon Photovoltaics

Characterisation, Modelling and Simulation

https://doi.org/10.52825/siliconpv.v3i.2683

Published: 20 Jan. 2026

Contactless Measurement of Current-Voltage Characteristics of Back-Contact Solar Cells

Johannes M. Greulich[1,*], Cyril Leon[2], and Stefan Rein[1]

[1]Fraunhofer-Institute for Solar Energy Systems, Freiburg, Germany

[2]Fraunhofer-Institute for Solar Energy Systems, Freiburg, Germany. Now with Université Grenoble Alpes, CEA, LITEN, INES, Le Bourget du Lac, France

*Correspondence: Johannes M. Greulich, johannes.greulich@ise.fraunhofer.de

Abstract. This study presents the application of a novel contactless method for measuring the current-voltage characteristics to interdigitated back contact (IBC) solar cells, addressing challenges associated with the rear metal contacts. The method involves a comprehensive characterization approach, utilizing reflectance and different photoluminescence measurements including partial illumination and different excitation wavelengths. Conventional contacted flash test measurements serve as a comparison. By implementing a simplified procedure with only two wavelengths for EQE, this technique enables accurate performance characterization without direct contact to the cell, reducing the risk of cell damage and measurement time. Results show a good average agreement with a strong correlation between contactless and traditional methods, particularly for the open-circuit voltage (Bravais-Pearson correlation R = 0.98) and efficiency (R = 0.78), while highlighting some discrepancies in the measurements of the short-circuit current density and the series resistance R_s, which may result from both the contacted and the contactless measurement. The pixel-wise application of the R_s determination offers insights into the lateral distribution of series resistance-induced losses and highlights opportunities for optimizing cell design. This research confirms the efficacy of the adapted contactless method for IBC cell characterization and demonstrates its potential for broader applications, especially in inline measurement processes. Further refinements can enhance the absolute accuracy of the method.

Keywords: Contactless Measurement, IBC Solar Cells, Current-Voltage Characteristics

1. Introduction

Since several years, efficiency records for single-junction silicon solar cells are obtained with IBC (Interdigitated Back Contact) cell architectures and the current record of 27.3% of efficiency is being held by such a device [1]. Back-contact cells present a specific challenge in determining the performances since both metal contacts are located at the back of the device [2]. Modern interconnection technologies allow to omit the rear busbars, which further complicates the contacting for measuring the current-voltage (*IV*) characteristics. Recently, an approach to determine the *IV* characteristics of a device in a contactless way was proposed [3]. Such a method is particularly convenient to measure cells without metallization or with a complex metallization structure that would normally require the development of a specific contacting unit. It also decreases the risk of damaging the cell and can reduce the measurement time, which is particularly important for inline measurements in a running production facility.

In this study, we present an adaption of this contactless method to measure the performance of IBC cells. First, the approach and a description of the experimental setups are introduced. Then, measurements using the contactless approach are described and compared with the usual contacted method showing that the adapted contactless method can be used to characterize IBC performances.

2. Methodology

The contactless determination of the *IV* characteristic can be broken down into several steps, which are described in the following along with the experimental setups.

The reflectance spectrum of the cells is measured between 300 nm and 1200 nm with a step size of 20 nm on a golden chuck using the photospectrometer with an integrating sphere implemented in the commercially available LOANA tool from PVtools GmbH (Germany).

The relative External Quantum Efficiency (EQE) is determined by measuring the average photoluminescence (PL) signals of the cell at different wavelengths of the excitation light [4]. In our case, we use a very simplified approach compared to Ref. [3] with an 808 nm and a 450 nm laser only. PL signals are detected with the “modulum” setup, a commercial luminescence measurement system developed by Fraunhofer ISE and manufactured by Intego GmbH, (Germany) [5].

The absolute EQE is obtained using the following approach combining four elements: (i) the measured reflectance spectrum to account for reflection losses; (ii) the transmission and absorption spectra of the device, which are simulated assuming the Lambertian light-trapping equation [6] to account for transmission, parasitic absorption at the rear surface and escape light losses; (iii) the relative EQE measured at 808 nm and 450 nm that are scaled to absolute values assuming ideal internal quantum efficiency at 808 nm, i.e. IQE(808 nm) = 100%, hence assuming no recombination at 808 nm illumination, but accounting for parasitic absorption and recombination at 450 nm, and (iv) the parasitic front film absorption that is implemented assuming the properties of a dielectric front layer [7] and scaled to match the absolute EQE at 450 nm. By combining the measurements at 450 nm and 808 nm with the models for light-trapping and for parasitic absorption, we describe the EQE curve in the spectral range between 300 nm and 1200 nm. The data and procedure are exemplarily shown in Figure 1 for one cell.

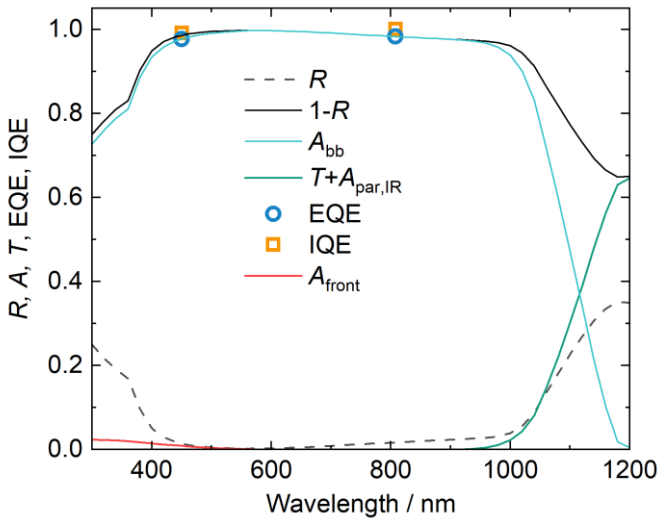

Figure 1. *For the determination of the charge carrier generation A_{bb}, we combine the measured reflectance spectrum R and the measured relative EQE at 450 nm and 808 nm with a light-trapping model for escape light and transmission T and parasitic absorption $A_{par,IR}$ in the infrared and a model for the parasitic absorption in the front films A_{front} for the UV and blue light.*

The short-circuit current density (J_{sc}) is then calculated using the band-to-band absorption A_{bb} and the standard AM1.5g solar spectrum.

The pseudo-*IV* curve is measured using Suns-PL calibrated to the open-circuit voltage [8]. For these measurements, we use the same camera and the same 808 nm laser as for the relative EQE step. From the J_{sc} at 1 sun, which is determined as described in the previous paragraphs, and the illumination intensity, we calculate the $J_{sc}(iV_{oc})$ curve. This curve is shifted to have a current density at $V = 0$ of J_{sc} at 1 sun.

The series resistance (R_s) is measured from PL measurements as described in [3, 9]. This includes two partially shaded and one homogeneously illuminated PL images. A specific shadow mask has been designed and PL images have been measured using the same camera and 808 nm laser as for the relative EQE step. The shadow mask (see Figure 3a) is designed to match the number of soldering pads on the cell's busbars and to generate the same current pattern for the contactless measurements that is expected in the module at maximum power point. The two partially shaded PL images are recorded with the shadow mask in two inverted positions. The equation to determine R_s is also applied pixel-wise to determine an image of R_s (see Figure 3b).

The *IV* or *J(V)* curve is then finally obtained by combining the series resistance with the $J_{sc}(iV_{oc})$ curve. The implied voltage of the $J_{sc}(iV_{oc})$ curve is reduced by the voltage drop at the series resistance to obtain the voltage of the illuminated *J(V)* curve: $J = J_{sc}$, $V = iV_{oc} - J_{sc} \cdot R_s$.

In this study, 150 high quality M10-sized IBC cells are characterized. The metallization is designed in a half-cell layout with 9 (10) n-type and 10 (9) p-type busbars in one half-cell (and the other). There are 14 solder pads per busbar, so 133 solder pads in total per full cell and polarity. 3 groups (labelled L for low, M for medium and H for high) are distinguished by the cell producer corresponding to different quality ranges of the cells. All IBC cells have been measured both, with the contactless approach described above at Fraunhofer ISE and in a contacted way for comparison using a flasher from halm elektronik GmbH, Germany at the cell producer's site.

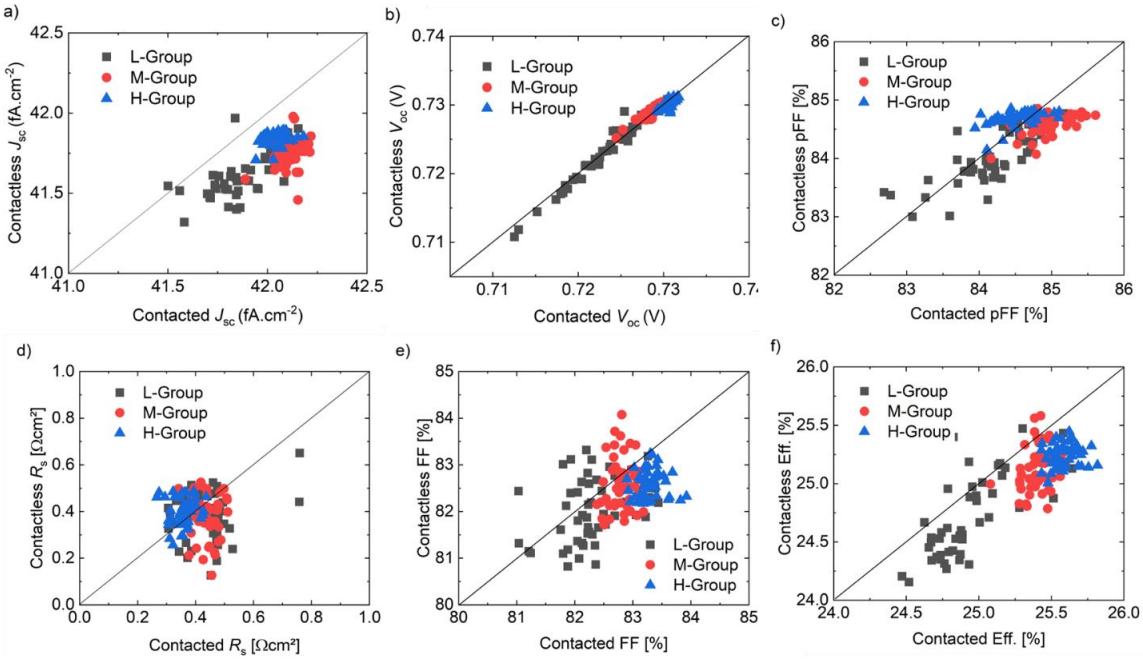

Figure 2. *Comparison of the performance parameters measured with the contactless and the contacted approach. For clarity, the x=y line is also shown as a black line in every graph.*

3. Results

The comparison of the values measured with the contactless and the contacted approach is shown in Figure 2.

Short circuit current (J_{sc}): The contactless data show the expected same overall trend as the contacted data, with a Bravais-Pearson correlation of R = 0.64, but with two main differences: (i) A slight offset of about 0.25 mA/cm² to lower values, which may be caused by the calibration of the contacted flasher and/or by the simplified approach to determine the J_{sc} contactlessly with only two wavelengths for the EQE. (ii) The cells from the M-Group show higher average contacted J_{sc} than the cells from the H-Group, while the opposite behaviour is observed for the contactless measurement.

Open circuit voltage (V_{oc}): an excellent agreement of both methods is obtained within the whole voltage range from 712-733 mV (RMS error 0.7 mV, R = 0.98).

Pseudo-fill factor (pFF): The trend is relatively similar between the two measurement methods (R = 0.71) and the quantitative agreement is acceptable (RMS error 0.37%$_{abs}$). However, we observe that the M-Group shows higher pFF than the H-group when measured in a contacted way and similar pFF when measured with the contactless method. Moreover, the pFF spread of the H-group is more pronounced when being measured contacted than contactless, potentially caused by hysteresis effects that are expected to be most pronounced for this group with highest open-circuit voltages.

Series resistance (R_s): Values obtained with both approaches agree well on average but show a significant scattering (R = 0.03). The contactless R_s image (Figure 3b) shows increased series resistance at the ends of the busbars, both at the top and bottom wafer edges and at the half-cell cutting edge.

Fill Factor (FF) and efficiency: Finally, observations on these two parameters follow the conclusions of the previous points. Indeed, we can observe a clear correlation (R = 0.78) with a slight offset between the contactless and contacted efficiency, mostly coming from the observed J_{sc} offset. Also, contactless FF and efficiency for the H-group are slightly lower when measured without contact, since the average R_s for this group was found to be slightly higher when measured with the contactless method.

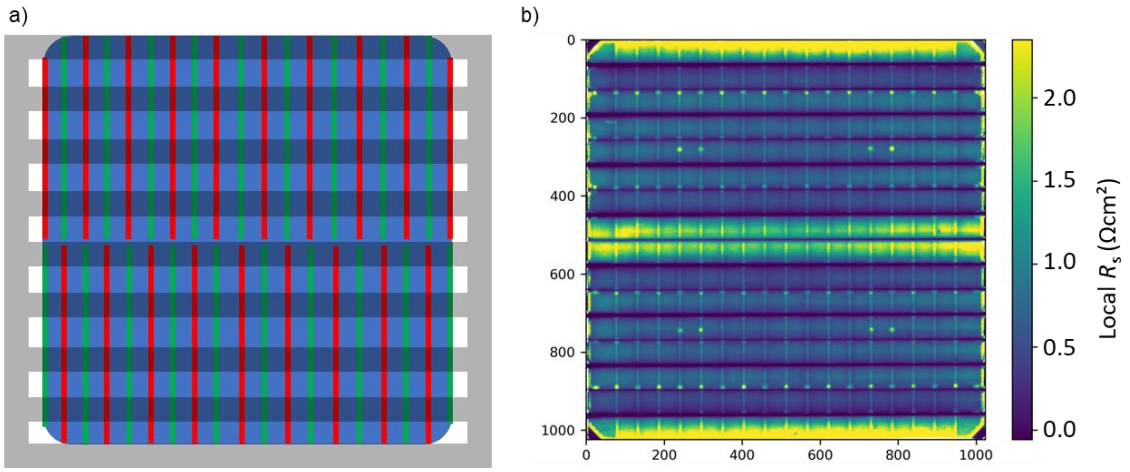

Figure 3. *a) Sketch of the setup for partially shaded PL imaging with the cell (blue area) with 19 vertically oriented busbars (red lines for n-type, green lines for p-type polarity) including the busbar interruption for half-cell cutting, and the shadow mask pattern (9 grey horizontal stripes). b) R_s image of one of the studied samples determined by the contactless shadow-mask approach. The black horizontal lines in Figure 3b simply represent the area excluded from analysis due to overlapping shadow mask positions.*

4. Discussion

The observed offset in J_{sc} (0.25 mA/cm²) is within the typical uncertainty range of 1-2% that can be expected for calibrated measurements in calibration laboratories. The offset could be further reduced with an additional calibration step. Excellent agreement for the open-circuit voltage can be achieved in terms of both, absolute agreement and low scattering. For the R_s, an excellent agreement of the average values is achieved. The scattering in the R_s data possibly originates partly from the contacted measurement at the cell's production site (reproducibility of contacting resistance, contact pattern, incomplete correction of hysteresis during fast *IV* scan) and partly from the contactless measurement (image noise, placement of shadow mask, reproducibility / stability of laser intensity). An automatized placement of the cells and the shadow mask might reduce the scattering of the data. Further research focusing on the R_s obtained with both approaches could be of a great help to improve the accuracy of the measured data in the future.

The analysis of contactless R_s images obtained by applying the equations pixelwise and assuming independent diodes (one example is shown in Figure 3b) gives insights into the lateral distribution of R_s-induced losses. The series resistance is increased at the half-cell edges because of the longer distance the current has to flow in the busbar there compared to the cell's center. In the cell's center, the current flows through the busbars only a length corresponding to half the distance of the solder pads, while this length is effectively larger (~2x) at the cell's edges. This highlights some room for improving the positions of the solder pads for higher module performance.

5. Conclusion

We have compared a contactless approach for characterizing interdigitated back-contact solar cells with conventional contacted flash testing. The approach is still in an early development stage, and the data shown here is based on offline measurements. Nevertheless, it shows a good relative and absolute agreement, while some room for improvement remains for an absolute interpretation of some parameters. Small adjustment may need to be done in order to correct the observed offsets. The contactless series-resistance imaging allows to identify further room for device improvement. Even without these small adjustment steps, the method already shows impressive efficiency and practicality for the characterization of IBC devices and appears promising for wider use in particular for inline applications.

Data availability statement

The datasets generated during and/or analysed during the current study are available from the corresponding author on reasonable request.

Author contributions

Johannes M. Greulich: Conceptualization, Investigation, Methodology, Supervision, Validation, Visualization, Writing – original draft

Cyril Leon: Data curation, Formal analysis, Investigation, Methodology, Software, Validation, Visualization, Writing – original draft

Stefan Rein: Funding acquisition, Project administration, Resources, Supervision, Writing – review & editing

Competing interests

The authors declare that they have no competing interests.

Funding

This work is supported by Fraunhofer-internal funding.

References

[1] M. A. Green, E. D. Dunlop, M. Yoshita, N. Kopidakis, K. Bothe, G. Siefer, D. Hinken, M. Rauer, J. Hohl-Ebinger, and X. Hao, “Solar cell efficiency tables (Version 64),” Prog Photovolt Res Appl., vol. 32, no. 7, pp. 425–441, 2024, doi: https://doi.org/10.1002/pip.3831

[2] M. Glatthaar, J. Hohl-Ebinger, A. Krieg, M. Greif, L. Greco, F. Clement, S. Rein, W. Warta, and R. Preu, “Accurate IV-Measurement for Back Contact Solar Cells,” in: 25th European Photovoltaic Solar Energy Conference and Exhibition, Valencia, Spain, 2010, doi: https://doi.org/10.4229/25thEUPVSEC2010-2CV.3.13

[3] J. M. Greulich, W. Wirtz, H. Höffler, N. Wöhrle, M. K. Juhl, O. Kunz, S. Rein, and A. W. Bett, “Contactless measurement of current-voltage characteristics for silicon solar cells,” Sol. Energy Mater. Sol. Cells, vol. 248, p. 111931, 2022, doi: https://doi.org/ 10.1016/j.solmat.2022.111931

[4] M. K. Juhl, M. D. Abbott, and T. Trupke, “Relative external quantum efficiency of crystalline silicon wafers from photoluminescence,” IEEE J. Photovolt., vol. 7, no. 4, pp. 1074–1080, 2017, doi: https://doi.org/10.1109/JPHOTOV.2017.2697313

[5] O. Fischer, A. D. Bui, F. Schindler, D. Macdonald, S. W. Glunz, H. T. Nguyen, and M. C. Schubert, “Versatile implied open-circuit voltage imaging method and its application in monolithic tandem solar cells,” Prog Photovolt Res Appl., vol. 33, no. 1, pp. 40–53, 2025, doi: https://doi.org/10.1002/pip.3754

[6] M. A. Green, “Lambertian light trapping in textured solar cells and light-emitting diodes: Analytical solutions,” Prog Photovolt Res Appl., vol. 10, no. 4, pp. 235–241, 2002, doi: https://doi.org/10.1002/pip.404

[7] S. Duttagupta, F. Ma, B. Hoex, T. Mueller, and A. G. Aberle, “Optimised Antireflection Coatings using Silicon Nitride on Textured Silicon Surfaces based on Measurements and Multidimensional Modelling,” Energy Proced., vol. 15, pp. 78–83, 2012, doi: https://doi.org/10.1016/j.egypro.2012.02.009

[8] T. Trupke, R. A. Bardos, M. D. Abbott, and J. E. Cotter, “Suns-photoluminescence: Contactless determination of current-voltage characteristics of silicon wafers,” Appl. Phys. Lett., vol. 87, no. 9, p. 93503, 2005, doi: https://doi.org/10.1063/1.2034109

[9] H. Höffler, W. Wirtz, J. M. Greulich, and S. Rein, “Quantitative contactless determination of the series resistance of silicon solar cells,” in 38th European Photovoltaic Solar Energy Conference and Exhibition, Online, 2021, pp. 233–236, doi: https://doi.org/10.4229/EUPVSEC20212021-2CV.1.5